PAPER A

MIGRATION OF THE KING MOUNTAIN DATASET

Le-Wei Mo

ABSTRACT

In this paper, I describe application of prestack Kirchhoff depth migration to the King Mountain cross-well field data set. The data preprocessing consists of tube wave attenuation, amplitude restoration and tapered muting of the direct arrivals. The velocity model used in migration is the transmission travel time tomogram. Migration images show generally good alignment of the image events at common lateral location image profiles. The misalignments are owing to the fact that the travel time tomogram does not sufficiently model the travel time kinematics of the geological diffractors. I correct this misalignment using a maximum energy stack method. The final migration image reveals a reef structure which is not observable in surface 3-D seismic surveys, and the migration image is in general consistent with results obtained by other independent processing methods.

INTRODUCTION

In the past few years, there have been technology advancements in cross-well seismic data acquisition; the well separation distance that can be safely surveyed has increased from a few hundred feet to over a thousand feet. There are also technology advancements in cross-well data processing as well. In this paper, I apply prestack Kirchhoff depth migration to the King Mountain cross-well field data set. In this data set, the geology is fairly complicated to call for the application of migration imaging. Kirchhoff depth migration does not have dip limitations in its imaging capability, so it can generally image complicated geology setting quite well. Also, because Kirchhoff migration is a summation process, it can deal with noisy seismic data by adaptive summation better than reverse-time migration.

In this paper, I will go over the steps that I used to process the King Mountain cross-well data set. The processing steps include preprocessing of field data, common shot gather migration, correcting misalignment in prestack migration images and stack.

PREPROCESSING

The data set has 201 shots and 203 receivers, source and receiver sampling intervals are both 5 ft. The record time sampling interval is 2.5 ms, the record length is 180 ms. The interwell separation distance is 640 ft. Because both the source and receiver wells have a perforation in the depth range of the survey, these perforations excite strong tube waves in both the source and receiver wells. Intensive preprocessing is first needed to attenuate the tube waves (Mo and Harris, 1995). The tube wave attenuation method applies the physical wave propagation process of the source and receiver tube waves. The source well tube waves are well sampled in the common shot gather data. It aligns and stacks the source well tube waves in CSGs to estimate the source well tube waves. The estimated source well tube waves are then subtracted from the CSG data. Then, it applies the same method to attenuate the receiver tube waves in common receiver gathers. Figure 1 is a common shot gather after attenuation of both source and receiver well tubes.

Because our migration method operates in two-dimensions, but the field data are actually recorded in three-dimensions, the geometrical spreading amplitude difference is $\sqrt{r}$, where r is the propagation distance proportional to travel time in a constant velocity medium. I multiply each trace by the square root of the direct arrival travel time to correct for the 2-D to 3-D geometrical spreading difference. To correct the instrument amplitude inconsistency between the different traces, I estimate the amplitude of the direct arrivals in each trace, then normalize the whole trace by the direct arrival amplitude. Figure 2 is the resulting common shot gather data after the above amplitude corrections. Next, the direct P-wave arrivals are attenuated by tapered muting, and the data are ready for P-wave data migration.

KIRCHHOFF MIGRATION

The exact formula Kirchhoff migration is derived based on a homogeneous medium. Then the formula is extended to be used in heterogeneous media. We begin with the Helmholtz equation:

$$(\nabla^2 + \omega^2 / v^2)P = \delta(r - r_0) \tag{1}$$

The wave field is back propagated from the recording surface into the medium and is reconstructed by the Kirchhoff integral:

$$P(r,\omega) = 2\int_S P(r_g,\omega)\partial_n G dS \tag{2}$$

where $G = A(r \mid r_g)e^{-i\omega\tau(r|r_g)}$ is the WKBJ Green's function from the receiver. The reflectivity is estimated by dividing the reconstructed wave field to the source wave field:

$$R(r,\omega) = \frac{P(r,\omega)}{P_s(r,\omega)} \tag{3}$$

The source wave field is also approximated by the WKBJ Green's function, $P_s(r,\omega) = A(r \mid r_s)e^{-i\omega\tau(r|r_s)}$. After applying the inverse Fourier transform to the equation (3), we obtain the the Kirchhoff integral formula for migration. The migration formula for a single source is:

$$R(r) = \int_S \frac{A(r|r_g)}{A(r|r_s)} \frac{\cos\theta_g}{v_g} \partial_t P(r_g, \tau(r \mid r_s) + \tau(r \mid r_s))dS \tag{4}$$

where R is the migration reflectivity, A is the geometrical spreading amplitude from the source or from the receiver to a diffraction point, v is velocity, P is the common source seismic data, θ_g is takeoff angle at the receiver, and τ is the direct arrival travel time from the source or receiver to the diffraction point, the integration is done over the receivers. Migration reflectivity estimation by this formula has the property that their relative magnitudes are preserved. It is very important for lithology identification. When

the size of the features are small, their presence can only be noticed by using amplitude. I use the finite-difference method to solve the Eikonal equation to obtain the travel time imaging conditions (Mo, 1996). The geometrical amplitude weighting factors are calculated by an approximation method (Vidale, 1991). Figure 3 is the migration image of the common shot gather data in Figure 2. As is typical in cross-well prestack migration images, the remnant direct arrivals left from the preprocessing tapered muting image at the physical source-creating artifacts centered at the source. The source imaging artifacts must be muted before the individual images are stacked. The travel time tomogram models the kinematics of the direct arrivals quite well, as is obvious from the fact that the direct arrivals are strongly focused at the physical source. But the travel time tomogram -- the velocity model I used in the migration, may not model the kinematics of the geological diffractions sufficiently.

COHERENT STACKING OF THE IMAGES

After migration of all the common shot gathers, we have an image volume. Each image in the volume covers the same interwell section. But depending on the relative orientations of the geology strata and the incidence direction of the sources, individual images might image some places better than elsewhere. Figure 4 shows the common lateral location image profile at point mid-way between the wells. It is composed from the common lateral location image traces of all the prestack common shot gather migration images. The upper-left to lower-right diagonal area has the artifacts from imaging the physical source as a diffractor. Direct arrival travel time and diffraction travel time can have tangency intersections. Previously, I showed that the direct arrivals can not be muted too severely so as to preserve diffractions that are tangent to the direct arrivals. However, this image area around the physical source must be muted before stacking the migration images to produce the final image.

The image area above the diagonal line is from sources below the geological strata, and the image area below the diagonal line is from sources above the geological strata. Owing to the inaccuracy of the travel time tomogram in describing the diffraction kinematics, the image events in the above two triangular areas are not very well aligned horizontally. To solve this problem, I apply maximum semblance energy stack. First, a master trace is obtained from stacking the prestack common lateral profiles (Figure 4). Then, each trace in the profile is shifted up or down slightly to achieve maximum alignment for stacking. The semblance is computed by the following equation:

$$S = \frac{\sum_t (M_t + T_{t+i})^2}{\sum_t (M_t^2 + T_{t+i}^2)} \tag{5}$$

where M is the master trace and T is any one trace in the common lateral profile. The maximum semblance is selected, and the corresponding index i corresponds to the number of depth interval shift to be applied to the trace.

RESULTS

Since the field data are recorded by using frequency sweeps, the wavelets in the field data are zero phased. Kirchhoff integral migation transforms the zero-phased temporal wavelet into zero-phase spatial image wavelet. The peaks of the image wavelets are located at the geological interfaces which generate the reflections or diffractions. Depending on whether the sources are above or below the interfaces, and whether the interfaces are diffraction interfaces or reflection interfaces, the polarity of the image wavelets can be very complex. We can not simply add or subtract the images of sources above or below the interfaces, both lead to destructive interference of the images.

Thus, I took a compromise approach; I stacked the images having sources below the image area (the upper-right portion of Figure 4) and the images having sources above the image area (the lower-right portion of Figure 4). Finally the two resulting images are merged at the depth of 8600 ft. Figure 5 is the final stacked migration image. The image above 8600 ft is generally flat. Around the depth of 8800 ft, however there is an oval-shaped anomaly extending from the right well to a point just beyond midpoint between the wells. The image below the depth of 9000 ft is again flat. The image event at the depth of 9100 ft corresponds to an interface separating lower velocity upper strata from higher velocity lower strata. In the raw data, there are obvious head waves from this interface.

CONCLUSIONS

I have demonstrated the Kirchhoff depth migration process in the King Mountain data set. Cross-well travel time tomogram provides the background velocity, which has low resolution and is closer in property to the lithology rock physics parameters. Migration

reflectivity images provide higher resolution, but are further in property from the rock physics parameters. The migration image obtained is consistent with results obtained by other independent processing methods, such as travel time tomogram and CDP-mapping.

REFERENCES

Langan, R. T., Harris, J. M., Lazaratos, S. K., and Jensen, T. L., 1995, Crosswell seismic imaging in the Permian Basin: Vol. 6, No. 1, Paper U.

Mo, L., and Harris, J. M., 1995, Attenuation of tube waves in cross-well seismic survey: Expanded abstracts, 161-164, SEG meeting.

Mo, L., 1996, Calculation of direct arrival travel time by the Eikonal equation: Paper-H, STP, Vol. 7, No. 1.

Vidale, J., 1991, Rapid calculation of amplitude: Geophysics, 56, 880-884.

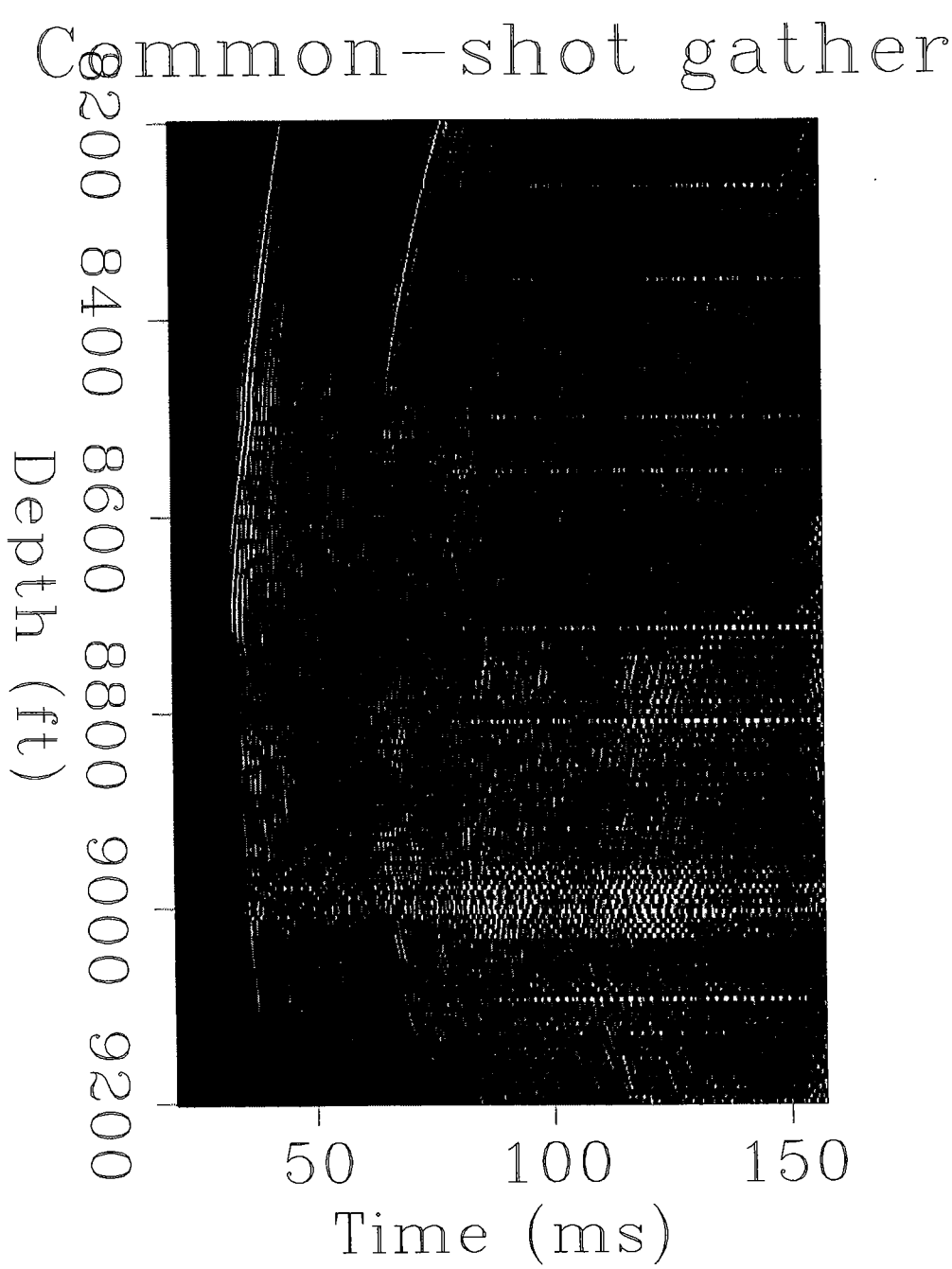

Figure 1. A common shot gather. This data has been subject to a tube wave attenuation process, which attenuates both source and receiver well tubes.

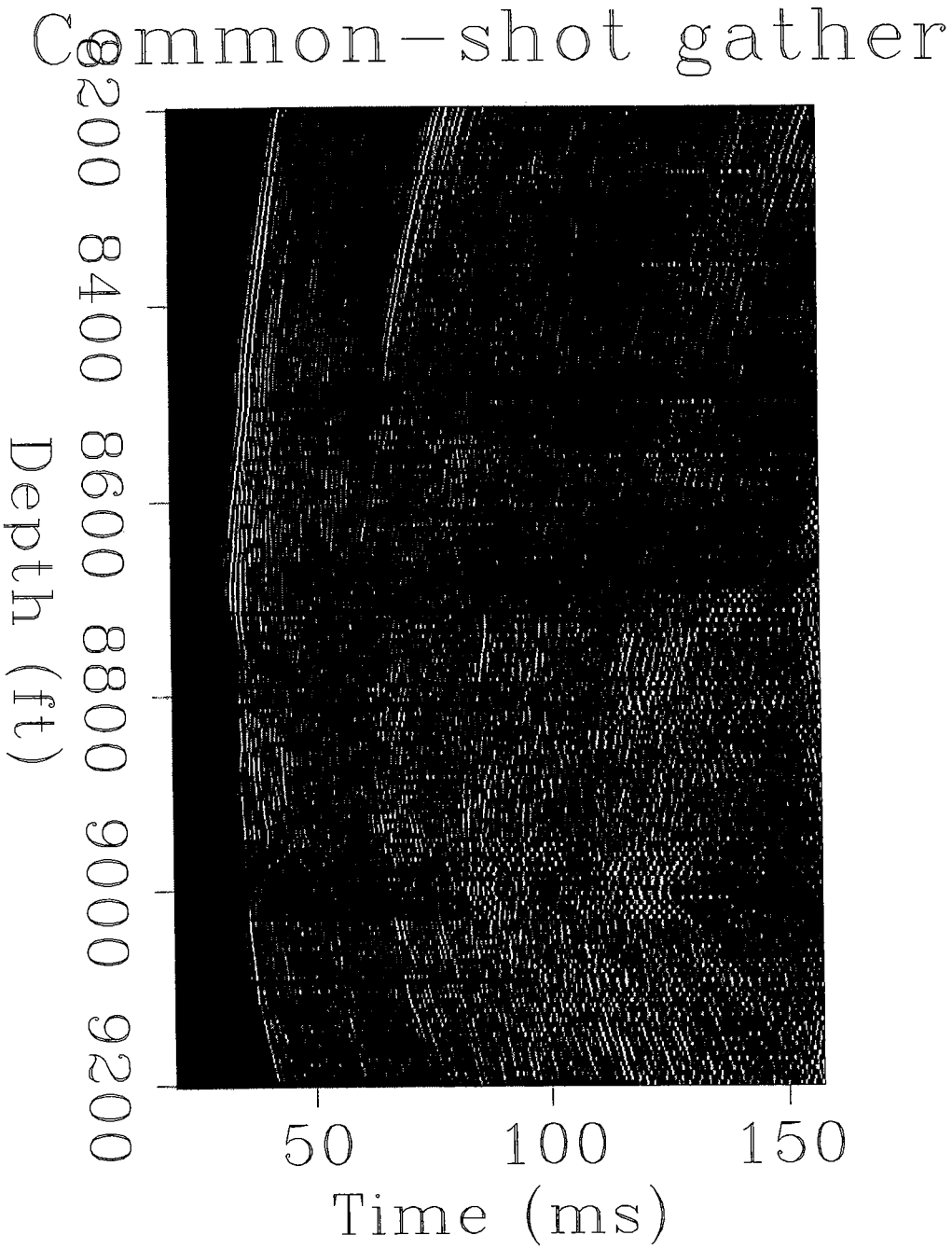

Figure 2. The previous common shot gather after amplitude adjustment to correct for 3-D to 2-D geometrical spreading difference and instrument amplitude anomalies.

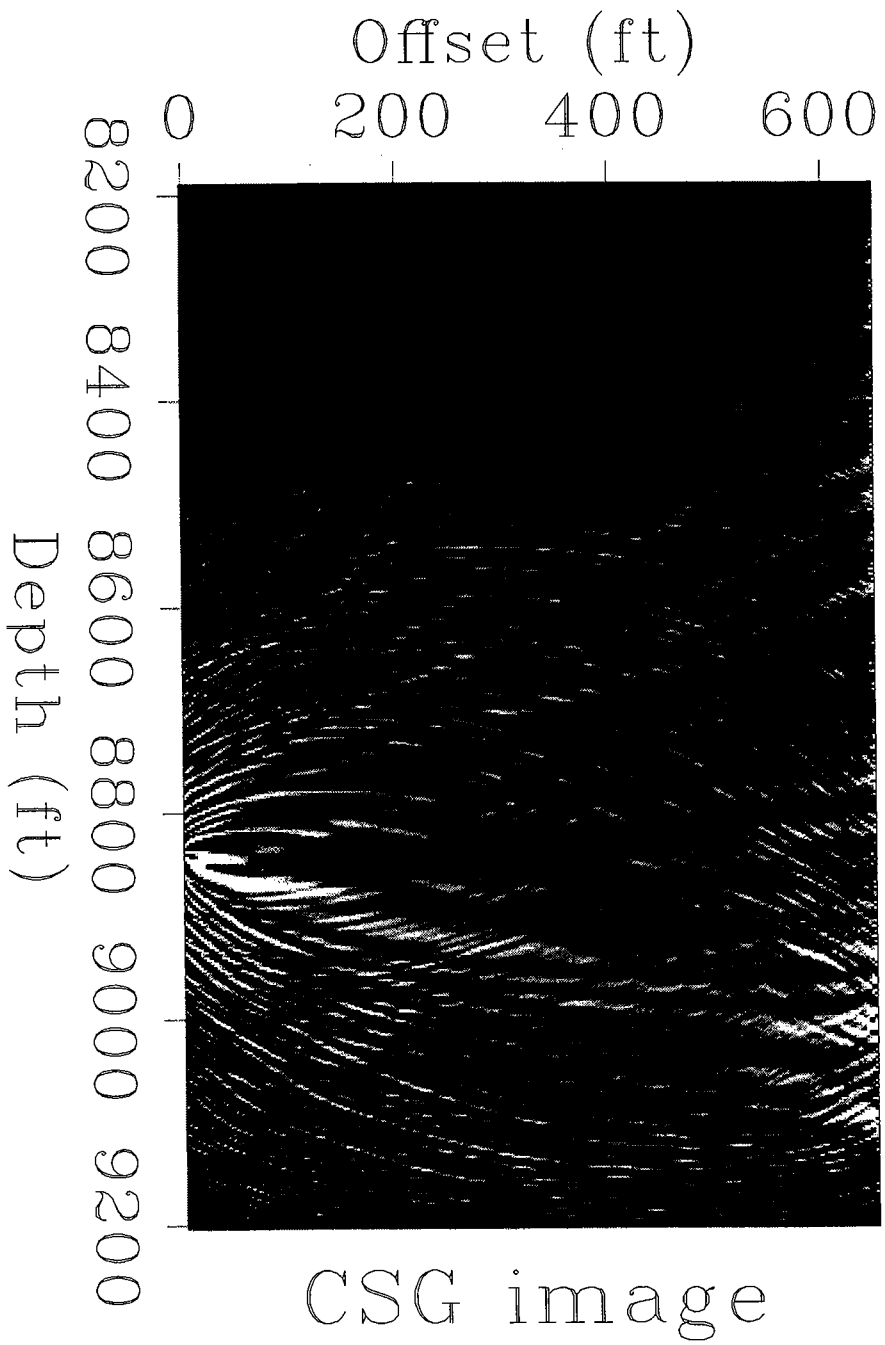

Figure 3. Common shot gather migration image of the data in Figure 2. The artifacts from imaging the physical source must be muted before the individual migration images are stacked.

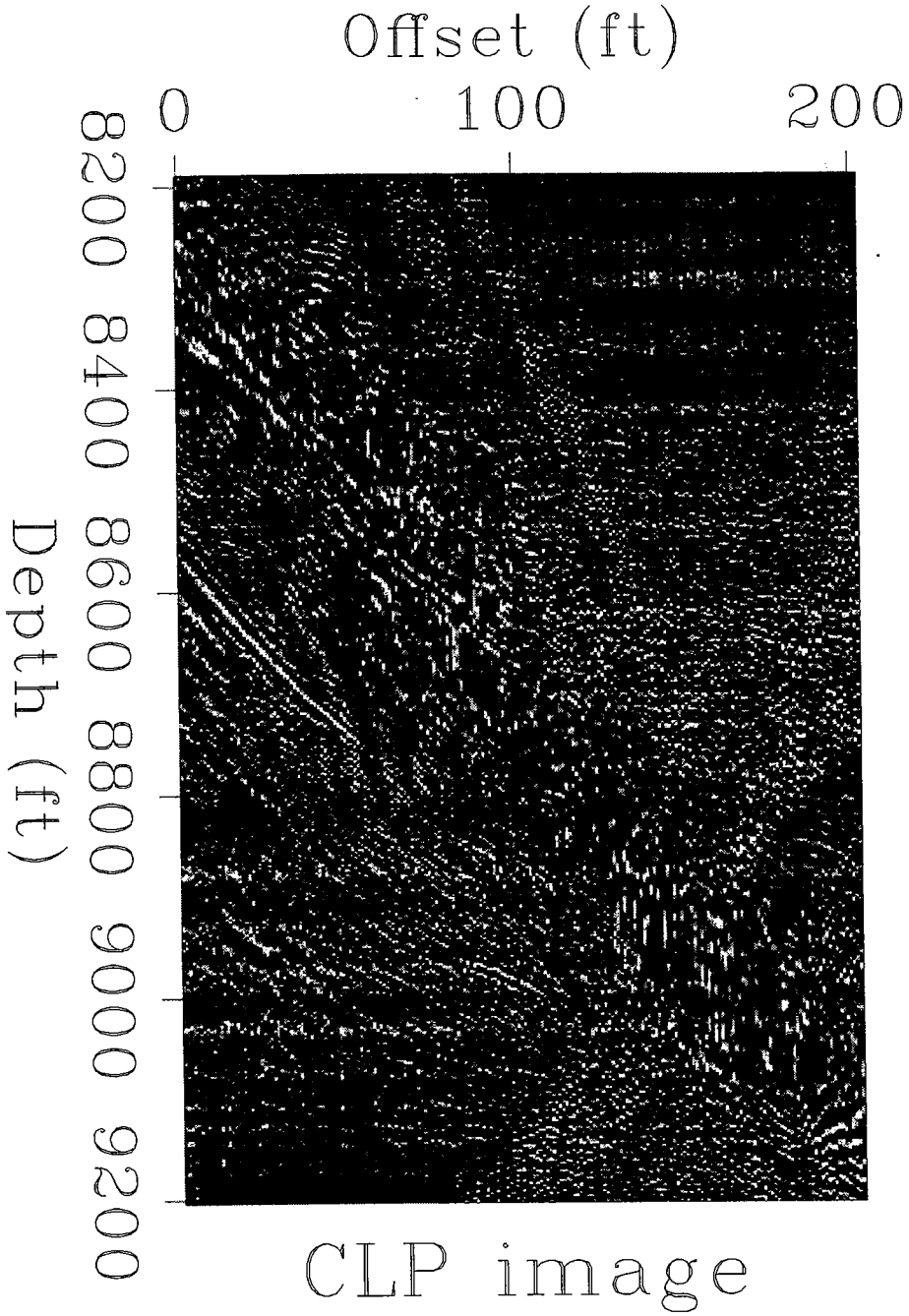

Figure 4. A common lateral location image profile at midpoint between the wells. The upper-left to lower-right diagonal shows the artifacts from imaging the physical sources by the direct arrivals. The misalignment of the image events are handled by maximum semblance energy stacking.

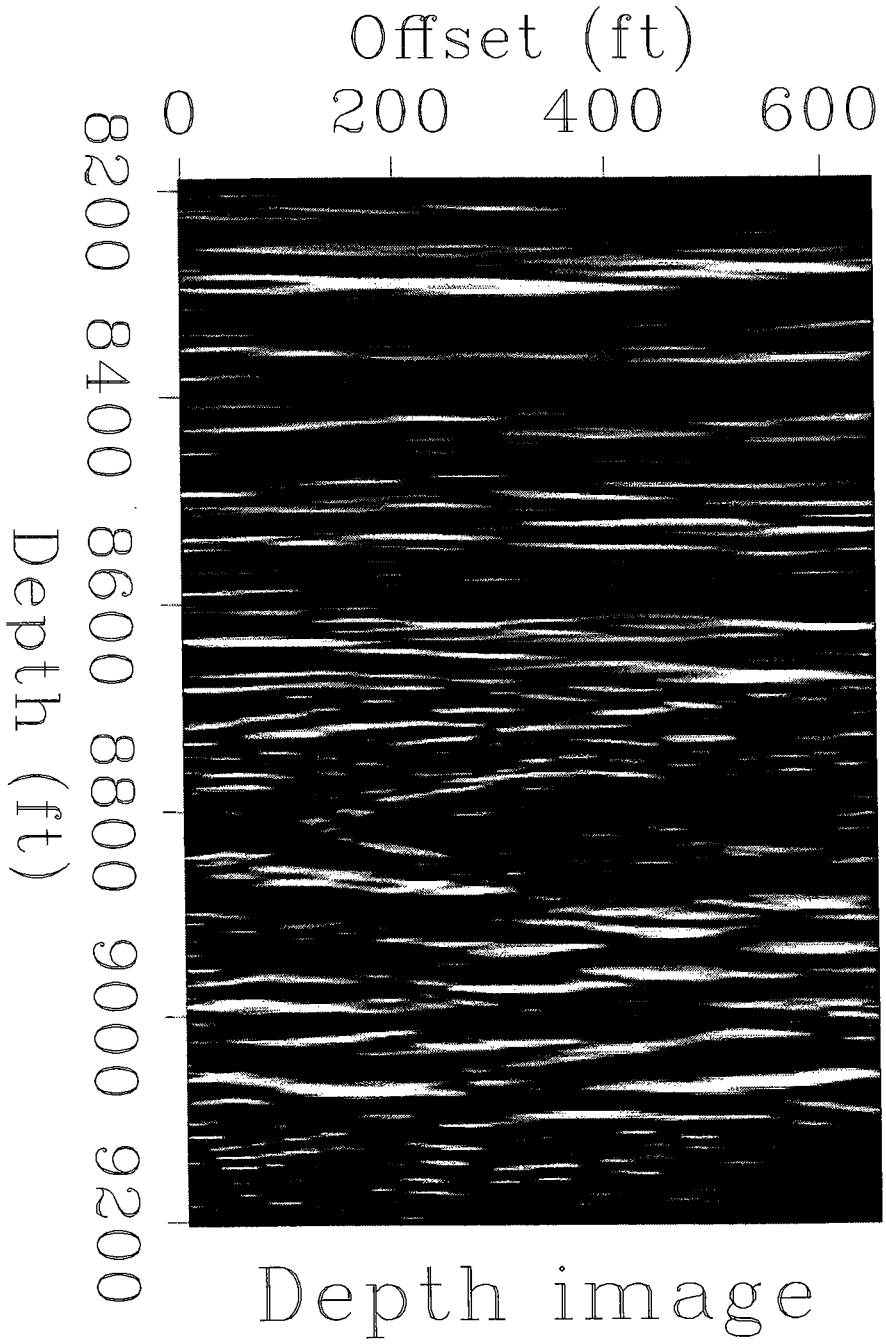

Figure 5. Final stack migration. The image events above 8600 ft are generally flat. At around the depth of 8800 ft, the oval-shaped anomaly corresponds to a reef. The image events below 9000 ft are again almost flat.